TERAHERTZ SPECTROSCOPY AND DENSITY FUNCTIONAL THEORY ANALYSIS OF THE MOLECULAR INTERACTIONS IN CRYSTALLINE OROTIC ACID MONOHYDRATE

Zh. Zheng*, F. Zeng, Y. Zhi, L. Zhu

School of Electronic Engineering at Xi'an University of Posts & Telecommunication, Xi'an, China; e-mail: zhengzhuanp@xupt.edu.cn

The terahertz (THz) absorption spectrum of orotic acid monohydrate in the crystalline phase was experimentally obtained by using THz time-domain spectroscopy and computationally simulated by using density functional theory. Four distinct peaks were observed within the range of 12–128 cm^{-1}, and were computationally reproduced by simulations using the Perdew–Burke–Ernzerhof functional. A comparison of the experimental and calculated data indicated that the measured peaks mostly originated from intermolecular forces in which the interactions between orotic acid molecules dominated. In addition, the feature located at 110.2 cm^{-1} was attributed to the interactions between orotic acid and water molecules. These findings demonstrate that THz spectroscopy can be used to monitor molecular dehydration during industrial production.

Keywords: *terahertz time-domain spectroscopy, density functional theory, orotic acid monohydrate.*

ИССЛЕДОВАНИЕ МОЛЕКУЛЯРНЫХ ВЗАИМОДЕЙСТВИЙ В КРИСТАЛЛИЧЕСКОМ МОНОГИДРАТЕ ОРОТОВОЙ КИСЛОТЫ МЕТОДАМИ ТЕРАГЕРЦОВОЙ СПЕКТРОСКОПИИ И ТЕОРИИ ФУНКЦИОНАЛА ПЛОТНОСТИ

Zh. Zheng*, F. Zeng, Y. Zhi, L. Zhu

УДК 543.42

Школа электронной инженерии Сианьского университета почты и телекоммуникаций, Сиань, Китай; e-mail: zhengzhuanp@xupt.edu.cn

(Поступила 22 апреля 2021)

Терагерцовый спектр поглощения моногидрата оротовой кислоты в кристаллической фазе получен экспериментально и смоделирован с помощью теории функционала плотности. Четыре отчетливых максимума в диапазоне 12—128 см$^{-1}$ воспроизведены моделированием с использованием функции Пердью–Берка–Эрнцерхофа. Сравнение экспериментальных и расчетных данных показало, что измеренные максимумы появляются в основном из-за межмолекулярных сил, в которых доминируют взаимодействия молекул оротовой кислоты. Особенность при 110.2 см$^{-1}$ объяснена взаимодействием оротовой кислоты и молекул воды.

Ключевые слова: *терагерцовая спектроскопия во временной области, теория функционала плотности, моногидрат оротовой кислоты.*

Introduction. The terahertz (THz) waves of electromagnetic radiation lie between the microwave and far-infrared regions, within the frequency range of 0.1 to 10 THz. This frequency range is usually dominated by various resonances of intermolecular forces, such as hydrogen bonding and van der Waals forces, in crystalline solids [1, 2]. These forces guide the aggregation pattern of molecules in crystals. Therefore, one promising application of terahertz time-domain spectroscopy (THz-TDS) is the investigation of energy interactions in crystals [3].

Over the past few decades, technological advances in the generation and detection of THz radiation have facilitated various applications of THz-TDS [4–7]. Thus far, THz-TDS has been used in a number of fields for chemical characterization and biological detection because numerous organic molecules, such as saccharides and pyrimidine, have distinctive THz spectral fingerprints [8–10]. However, THz spectral inter-

pretation remains a challenging undertaking, the difficulty of which can be alleviated with technological innovations. As capabilities for computational complicated increase, investigations of complicated molecular systems become possible. Among the various theoretical methods, solid-state density functional theory (DFT) can be used to describe complex intermolecular forces [9, 10]. Therefore, robust spectral studies in the THz region can provide useful information on molecular interactions in crystalline solids.

Orotic acid monohydrate (vitamin B_{13}), the only effective precursor for the biosynthesis of pyrimidine nucleobases, was determined in 1973 [11]. In recent years, it has been used as a nutritional medicine to improve liver function and to promote the repair of liver cells. To elucidate its biochemical functions, spectral information on molecular interactions can shed light on biological interactions [9, 12, 13]. Although spectral analyses of orotic acid have been published [14, 15], to the best of our knowledge, THz spectral studies of orotic acid monohydrate have not been reported.

Herein, we report the room temperature (RT) THz absorption spectrum of orotic acid monohydrate within the frequency range of 12–128 cm^{-1}. To determine the contributions of intramolecular interactions, the absorption spectra of orotic acid monohydrate and its anhydrate were compared. We also applied solid-state DFT with periodic boundary conditions to characterize the molecular interactions. In summary, experimental and calculated spectral data were collected, spectral peaks were assigned, and the origins of these peaks were analyzed.

Experimental and theoretical methods. A powder X-ray diffraction (PXRD) experiment was performed at the Analytical Research Facility of Northwestern University. XRD patterns were recorded using a diffractometer (D/MAX-3C, Rigaku, Japan). Data were collected within the 2θ ranges from 5 to 50° using CuK_α radiation. The XRD data of a previous study [11] were obtained using Mercury software.

The THz spectrum was acquired at Capital Normal University using an in-house THz-TDS system with a spectral resolution of 2.0 cm^{-1} within the range 12–128 cm^{-1} [16]. In this system, the incident laser was produced by femtosecond pulses at 800 nm with a pulse width of 50 fs from a Ti:sapphire femtosecond laser amplifier operating at a repetition rate of 1 kHz. Specifically, the THz pulses were generated by using fundamental (800 nm) and second harmonic (400 nm) beams to excite the plasma in dry air. THz temporal signals were detected with electro-optical sampling [17].

Orotic acid monohydrate (CAS-number: 50887-69-9) was acquired from Xi'an Yobios Biological Technology Co. Ltd. The sample was analytical grade (>99%) and used without further purification. It was first crushed into a fine powder using a mortar and pestle to minimize particle scattering. Then, mixture of orotic acid monohydrate and polytetrafluoroethylene (PTFE) powders in the mass ratio of 1:4 was prepared and compressed into pellets 1.4 mm thick with a pressure of 600 kg/cm^2.

Theoretical calculations of the periodic systems were performed using the plane-wave density functional theory (PW-DFT) method within the generalized gradient approximation (GGA) [18]. Kleinman–Bylander norm conserving pseudopotentials and the Perdew–Burke–Ernzerhof (PBE) exchange–correlation functional were used [19]. The plane wave cutoff energy was set to 1000 eV. The total energy converged to 10^{-8} eV/atom, and the maximum force between the atoms was less than 10^{-5} eV/Å. In addition, the Γ-point was used to calculate the vibrational frequencies. The IR intensities of the normal modes were calculated from the oscillator strength to give the effective charges and the normal mode eigenvectors. The crystal cell parameters used for orotic acid monohydrate are as follows [11]: space group P-1 ($Z = 2$), $a = 5.899$ Å, $b = 6.929$ Å, $c = 9.592$ Å, $\alpha = 74.68°$, $\gamma = 72.32°$, $\beta = 68.45°$, and $V = 342.206$ Å^3. Figure 1 shows the molecular structure and molecular arrangement of orotic acid monohydrate.

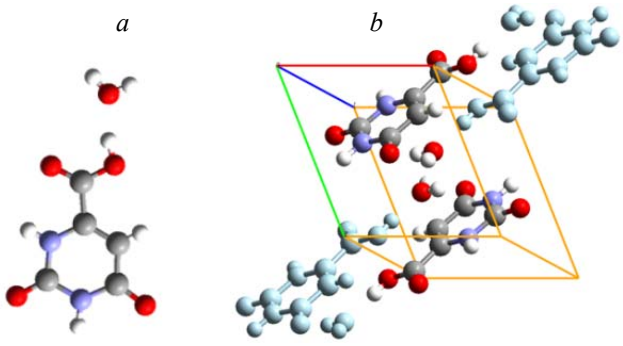

Fig. 1. The molecular structure (a) and molecular arrangement (b) of orotic acid monohydrate.

Results and discussion. The purity of the orotic acid monohydrate powder was verified by XRD Prior to conducting the THz experiments. The results are shown in Fig. 2a. As expected, orotic acid monohydrate has C_i crystal symmetry. Figure 2b shows the 2θ positions and the relative peak intensities, which have been reported [11]. The data obtained in experiment agreed with the previously reported data.

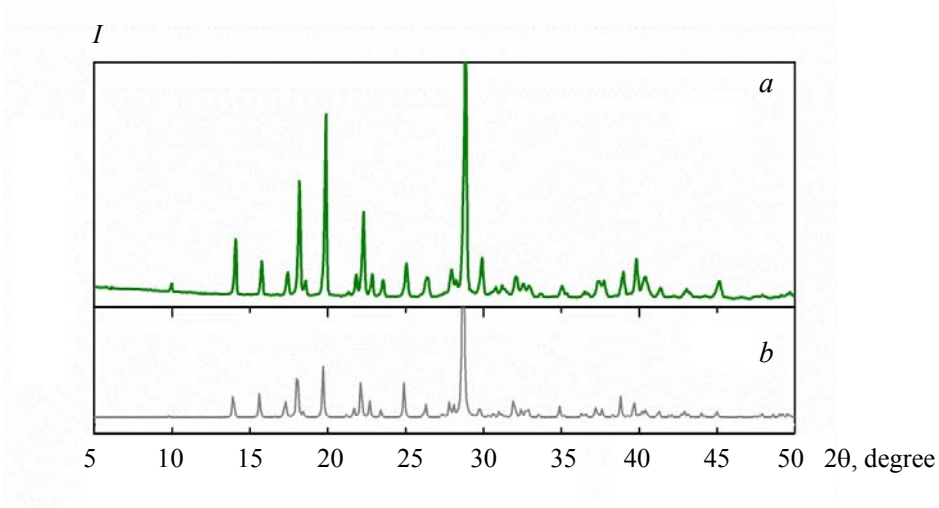

Fig. 2. Powder XRD pattern of orotic acid monohydrate (a) and previously published XRD (b) [11].

The RT THz absorption spectrum of orotic acid monohydrate is shown in Fig. 3 (label *1*). Four distinct absorption peaks were observed in the frequency range of 12–128 cm^{-1}, specifically at 83.0, 94.7, 110.2, and 120.0 cm^{-1}. Two relatively strong absorption peaks appeared at 83.0 and 94.7 cm^{-1}, and two medium absorption peaks were located at 110.2 and 120 cm^{-1}. Hernanz et al. investigated the vibrational spectrum of orotic acid, and the reported peak at 103 cm^{-1} was observed in our study [14]. In our previous study, orotic acid exhibited distinct THz absorption peaks at 88.3, 95.5, 116.7 cm^{-1} and a shoulder peak at 102.5 cm^{-1} (label *2*) [15]. As shown in Fig. 4, orotic acid monohydrate and its anhydrate clearly did not share the same absorption features. But the absorption peak at 94.7 cm^{-1} for orotic acid monohydrate was identified in the envelope of the peak at 95.5 cm^{-1} for orotic acid. Thus, the spectral features of orotic acid monohydrate obtained, except for the one at 94.7 cm^{-1}, originated from intermolecular interactions.

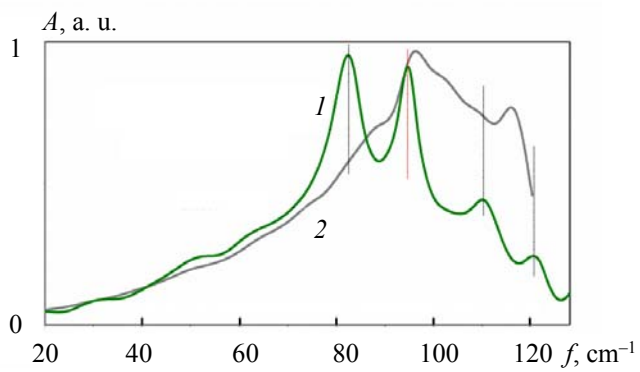

Fig. 3. The measured THz spectra of orotic acid monohydrate (*1*) and orotic acid (*2*).

To facilitate spectral interpretation, simulations were performed using solid-state theory with the unit cell as the starting point. As full optimization of the geometry reproduces structural parameters at absolute zero, the frequency values obtained with the fully optimized geometry are generally inadequate for comparisons with the RT THz spectrum [10]. Therefore, our calculations were optimized by fixing the unit cell, and the frequency of each normal mode was calculated using the harmonic approximation with the optimized geometry. According to the molecular parameters [11], a monohydrate unit cell of orotic acid crystal contains four molecules, including 36 atoms. This structure leads to 108 optical modes: $54A_u$+$54A_g$. Of these

modes, 84 correspond to intramolecular vibrations whereas the remaining 21 ($9A_u$+$12A_g$) can be attributed to intermolecular phonons. Vibrational modes with A_u symmetries are only infrared active because the point group of the unit cell possesses C_i symmetry.

Figure 4 shows the calculated results in red solid bars. Four optical modes were obtained within the range 12–128 cm^{-1}. A high quality of fit to the experimental data was obtained with the calculated data. Therefore, peak assignment was easily made, as shown in Table 1. In detail, the calculated modes at 93.8, 110.4, and 123.4 cm^{-1} corresponded to the observed features at 94.7, 110.2, and 120.0 cm^{-1}, respectively. However, the calculated mode at 66.4 cm^{-1} did not correspond to any experimental feature. This mode was likely the result of an overestimation of the system energy by solid-state theory [9].

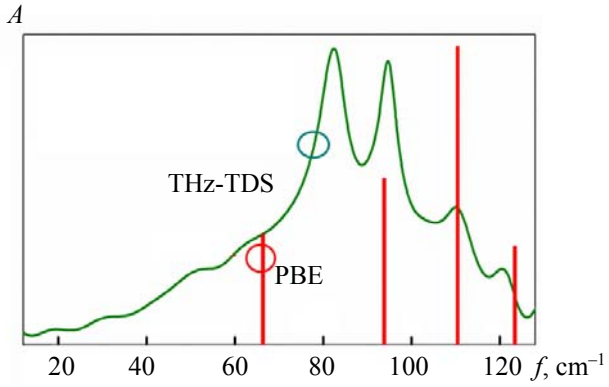

Fig. 4. The measured THz spectrum of orotic acid monohydrate is shown in line. Solid bars indicate the calculated frequencies, and the height represents the relative intensity.

On the basis of these assignments, the feature at 94.7 cm^{-1} was attributed to the out-of-plane bending of the phenyl and carboxyl groups around the crystal *b*-axis, the feature at 110.2 cm^{-1} was ascribed to in-plane optical rotation along the crystal *a*-axis, and the remaining feature at 120.0 cm^{-1} was determined to arise from optical rotation along the crystal *b*-axis. It should be noted that the calculated modes were characterized by visually inspecting the atomic displacements. Each mode was assigned to its dominant vibrational component. Table 1 lists the experimental and calculated spectral data. Discrepancies clearly existed between the calculated and experimental absorption intensities. These deviations were partly caused by the moderately rising baseline in the experimental spectrum. Additionally, the larger cutoff energy and appropriate correlation function for the simulations were likely chosen to obtain good correlation between the calculated and experimental spectral intensities [10, 18]. Moreover, the feature at 83.0 cm^{-1} was not reproduced by this simulation. Therefore, the simulation conditions of the solid-state theory were sometimes ineffective in accurately predicting the intermolecular forces of crystalline structures [9, 10].

TABLE 1. Experimental Features and Calculated Modes (cm^{-1}) of Orotic Acid Monohydrate with Molecular Interactions Unchanged and with Water Molecular Interactions Removed

Experiment	Calculation	
THz-TDS	with molecular interactions unchanged	with water molecular interactions removed
	66.4 (1.78) *	65.7 (1.36)
83.0	–	83.9 (9.62)
94.7	93.8 (2.68)	99.6 (5.07)
110.2	110.4 (4.80)	–
120.0	123.4 (1.59)	124.0 (17.44)

* Intensities (km/mol) are shown in parentheses.

Because two pairs of orotic acid and water molecules exist in the unit cell, the intermolecular interactions of orotic acid monohydrate may exist in three structural sub-units: orotic acid-orotic acid, water-water, and water-orotic acid. To determine the structural configuration of these intermolecular interactions, we performed separate simulations with water and orotic acid in the same unit cell with the same space group. Figure 5 shows the molecular arrangement of orotic acid monohydrate with different molecular interactions in the unit cell.

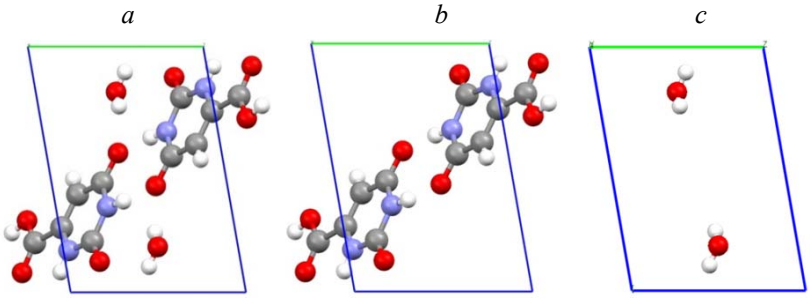

Fig. 5. The molecular arrangement of orotic acid monohydrate (a), orotic acid (b), and water molecules (c) in the unit cell.

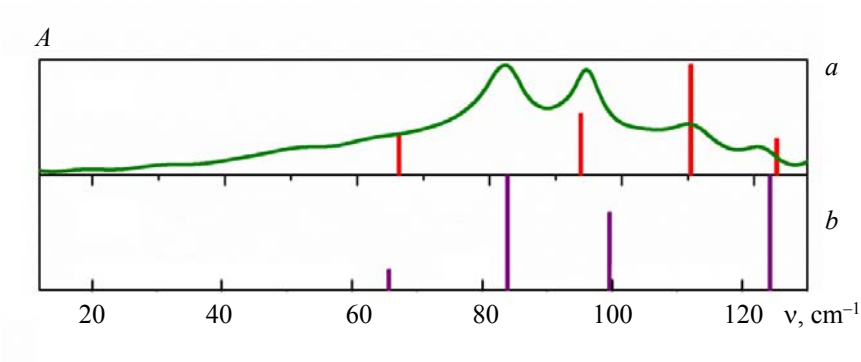

Fig. 6. The measured THz spectrum of orotic acid monohydrate compared with solid-state simulation results. Solid bars indicate the calculated frequencies and the height represents the relative intensity. Red (a): P-1 cell without water molecules; green (b): P-1 cell with orotic acid molecules.

The lowest-frequency vibrational mode of two water molecules was located at 252.7 cm^{-1}, indicating that the intermolecular forces between water molecules did not contribute to the measured features. Thus, only the calculated spectra based on the molecular models shown in Figs. 5a and b is shown in Figs. 6a and b as solid bars. Surprisingly, a calculated mode at 83.9 cm^{-1} was observed in one spectrum (Fig. 6b), indicating that the experimental peak at 83.0 cm^{-1} primarily originated from the intermolecular interactions between orotic acid molecules. The optical mode at 110.4 cm^{-1} was absent in the same calculated spectrum (Fig. 6b), indicating that the intermolecular interactions between orotic acid and water molecules mainly contributed to the measured feature at 110.2 cm^{-1}. This result suggests that THz-TDS may be used to monitor orotic acid monohydrate in dehydration processes [20]. Moreover, the peak located at 120.0 cm^{-1} was attributed to the interactions between orotic acid molecules from a comparison of the calculated data (Table 1). The feature at 94.7 cm^{-1} was attributed to a combination of intermolecular and intramolecular forces from a comparison of the calculated and experimental results and from a previous assignment of the peak at 95.5 cm^{-1} for orotic acid [15]. These peak assignments indicate that the measured absorptions mostly originated from the intermolecular forces between orotic acid molecules. Interestingly, the intensity of the two peaks at 120.0 cm^{-1} and 94.7 cm^{-1} was higher in spectrum (b) than in spectrum (a), indicating that the intra- and intermolecular interactions of orotic acid molecules were reduced in hydrates.

Conclusions. The THz spectrum of orotic acid monohydrate in the solid state was obtained, and four distinct peaks were observed within the range 12–128 cm^{-1}. Peak assignment was performed using the results of solid-sate DFT calculations. The measured features at 83.0 and 120.0 cm^{-1} primarily resulted from the interactions between orotic acid molecules. The feature at 94.7 cm^{-1} was attributed to a combination of

intermolecular and intramolecular forces. The remaining peak, at 110.2 cm^{-1}, was attributed to the interactions between orotic acid and water molecules. This peak can be used to monitor the dehydration of orotic acid monohydrate in industrial production.

Acknowledgements. This work was supported by the National Natural Science Foundation for Young Scientists of China (Grant No. 11604263) and the education department of Shaanxi Province (Grant No. 16JK1698). We thank Edanz (https://jp.edanz.com/ac) for editing a draft of this manuscript.

REFERENCES

1. Y. Ueno, K. Ajito, *Anal. Sci.*, **24**, 185–192 (2008).
2. L. Xie, Y. Yao, Y. Ying, *Spectrosc. Rev.*, **49**, 448–461 (2014).
3. M. Walther, B. M. Fischer, P. U. Jepsen, *Chem. Phys.*, **288**, 261–268 (2003).
4. Z. P. Zheng, W. H. Fan, H. Yan, *Chem. Phys. Lett.*, **525-526**, 140–143 (2012)
5. Z. X. Li, J. Zhou, X. S. Guo, B. B. Ji, W. Zhou, D. H. Li, *J. Appl. Spectrosc.*, **85**, 840–844 (2018).
6. Y. Ma, H. Huang, S. Hao, K. Qiu, H. Gao, L. Gao, W. Tang, Z. Zhang, Z. Zheng, *Sci. Rep.*, **9**, 9265 (2019).
7. E. M. Kleist, C. L. Koch Dandolo, J. P. Guillet, P. Mounaix, T. M. Korter, *J. Phys. Chem. A*, **123**, 1225–1232 (2019)
8. M. D. King, W. Ouellette, T. M. Korter, *J. Phys. Chem*., **115**, 9467–9478 (2011).
9. M. Takahashi, N. Okamura, X. Fan, H. Shirakawa, H. Minamide, *Phys. Chem. A*, **121**, 2558–2564 (2017).
10. P. U. Jepsen, S. J. Clark, *Chem. Phys. Lett*., **442**, 275–280 (2007).
11. G. Portalone, *Acta Crystallogr. E*, **64**, 0656 (2008).
12. J. Dong, Z. Zhang, H. Zheng, M. Sun, *Nanophotonics*, **4**, 472–490 (2015).
13. B. Lei, J. Wang, J. Li, J. Tang, Y. Wang, W. Zhao, Y. Duan, *Opt. Express*, **27**, 20541–20557 (2019).
14. A. Hernanz, F. Billes, I. Bratu, R. Navarro, *Biopolymer*, **57**, 187–198 (2000).
15. Z. P. Zheng, J. M. Gong, *J. Terahertz Sci. Electron. Inform. Techn.*, **17**, 425–438 (2019).
16. T. Chen, X. Wang, P. Han, W. Sun, S. Feng, J. Ye, Y. Xu, Y. Zhang, *J. Phys. D: Appl. Phys*., **52**, 455101 (2019).
17. Q. Wu, X. C. Zhang, *Appl. Phys. Lett*., **67**, 3523 (1995).
18. S. J. Clark, M. D. Segall, C. J. Pickard, P. J. Hasnip, M. J. Probert, K. Refson, M. C. Payne, *Z. Kristallogr.*, **220**, 567–570 (2005).
19. J. P. Perdew, J. A. Chevary, S. H. Vosko, K. A. Jackson, M. R. Pederson, D. J. Singh, C. Fiolhais, *Phys. Rev. B*, **46**, 6671–6687 (1992).
20. B. Zhang, S. Li, C. Wang, T. Zou, T. Pan, J. Zhang, Z. Xu, G. Ren, H. Zhao, *Spectrochim. Acta A: Mol. Biomol. Spectrosc.*, **190**, 40–46 (2018).